Springer

KSME

Journal of Mechanical Science and Technology 24 (12) (2010) 2587~2596
www.springerlink.com/content/1738-494x
DOI 10.1007/s12206-010-0916-0

Theoretical modeling and numerical solution of stratified condensation in inclined tubes †

Hamid Saffari* and Vahid Naziri

School of Mechanical Engineering, Iran University of Science and Technology, Tehran, 16846, Iran

(Manuscript received January 16, 2010; Revised August 14, 2010; Accepted August 31, 2010)

Abstract

The heat transfer phenomenon occurring during stratified condensation inside an inclined tube is investigated theoretically and numerically. Differential equations governing the kinematic, dynamic, and thermal aspects for vapor condensation inside inclined tubes, which are derived from a thin film flow modeling, are solved simultaneously. These solutions are achieved by applying an explicit finite difference numerical method to predict the condensation heat transfer coefficient variations along the tangential and axial coordinates. The inclination angle is found to have a significant effect on condensation heat transfer coefficient inside inclined tubes. In addition, in accordance with the given physical and thermal condition of working fluids, there is a specific optimum inclination angle. In this study, the 30°–50° range from the horizontal position is found to be the range of the optimum inclination angle for achieving the maximum condensation heat transfer coefficient, with R134a, R141b, and R11 as the working fluids. The results of the present study are compared with experimental data, and a good agreement is observed between them.

Keywords: Filmwise condensation; Heat transfer coefficient; Optimum inclination angle; Stratified flow; Theoretical investigation

1. Introduction

Condensing flow is one of the most common two-phase (vapor-liquid) flow regimes in industrial processes for refrigeration, desalination, and power generation, among others.

In general, condensation heat transfer is defined as the process by which a saturated vapor is converted into a liquid by removing the latent heat of condensation. From a thermodynamic standpoint, condensation occurs when the enthalpy of the vapor is reduced to the state of saturated liquid. In practice, the process is dynamic; heat must be transferred in order to achieve condensation. Thus, condensation occurs when a vapor comes in contact with a solid surface or a fluid interface whose temperature is below the saturation temperature of the vapor.

Heat transfer coefficient in condensation is, in general, much larger than that for convective heat transfer without a phase change. In addition, the difference in density of the vapor and the liquid remains large as long as the phase change takes place far away from the critical region. This causes strong buoyancy forces $(\rho_l - \rho_v)g$ to appear; thus, heat and mass transfer is supported by free flow [1].

Four basic mechanisms of condensation are generally recognized: dropwise, filmwise, direct contact, and homogeneous. Dropwise condensation occurs when condensation takes place on a surface that is not wetted by the condensate. Surface heat transfer coefficients for dropwise condensation (which occurs when the surface is wetted) are much higher than that for filmwise mode. However, providing and maintaining the non-wetting surface characteristics can be difficult; therefore, the condensate liquid (originally in the form of droplets) often gradually wets the surface, and drops coalesce to form a continuous liquid film with a corresponding reduction in thermal performance [2]. In direct contact condensation, the vapor condenses directly on the (liquid) coolant surface sprayed into the vapor space. Homogeneous condensation can eventually occur when vapor is sufficiently cooled below its saturation temperature, inducing droplet nucleation.

Much analytical and experimental research for film condensation has been performed since the pioneering work of Nusselt on laminar film condensation [3]. However, the development of technology requires a more compact and efficient heat exchanger for application in industries where condensation takes place inside inclined tubes, such as in liquefaction plants, air conditioners, and recently developed heat pipes and solar collectors.

Studies carried out on the subject of in-tube condensation can be divided into categories of laminar, wavy, or turbulent

† This paper was recommended for publication in revised form by Associate Editor Kwang-Hyun Bang
* Corresponding author. Tel.: +982177491228; Fax.: +982177240488
E-mail address: saffari@iust.ac.ir

flow; dropwise or filmwise condensation; free, forced, or mixed convection; plain or finned tube surface geometry; external or internal flow; horizontal, vertical, or inclined tube orientation; and condensation of pure vapor or mixture of vapors. This wide range of topics has been reviewed in the literature, such as by Cavallini et al. [4] and Dalkilic and Wongwises [5].

Wang and Rose [6] modified a model for condensation in inclined rectangular microchannels. In their research, the influence of inclination angle variation on the condensate film thickness around the channel inside the perimeter and the mean heat transfer coefficient along the channel length was addressed for square channels 0.5, 1.0, and 3.0 mm in size.

The influence of tube inclination on the flow regime boundaries of condensing steam was addressed in an experimental investigation performed by Nitheanandan and Soliman [7]. The effect of upward and downward inclinations within the different transition lines was discussed. Their study also showed that the zones occupied by the wavy and slug regimes experience significant shifts, whereas the effect on the annular flow boundary appear to be insignificant at the small inclination angles.

Fieg [8] and Hussein et al. [9] theoretically analyzed the laminar gravity-controlled film condensation heat transfer in inclined tubes. However, neither of these works considered the effect of the formation and growth of the stratified condensate layer at the bottom of the tube cross-section.

Han et al. [10] experimentally studied the improvement of heat transfer performance in inclined low-temperature closed thermosyphons with plain and internally grooved copper tubes. Three different working fluids were used with various volumetric liquid fill charge ratio. The results showed that working fluids, liquid fill charge ratio, the number of grooves, and inclination angle are crucial factors for the operation of thermosyphons. The range of the optimum inclination angle for this study was between 20° and 30° from the horizontal position.

Cho and Han [11] also conducted an experimental investigation aimed at a better understanding of the influence of the inclination angle and liquid charge ratio on condensation in closed two-phase thermosyphons with axial internal low-fins. As a result of the experimental investigation, the maximum heat flow rate in the thermosyphons was found to be dependent upon the liquid charge ratio and inclination angle, and that the inclination of the thermosyphon has a notable influence on condensation. In addition, the overall heat transfer coefficients and the characteristics at the operating temperature were obtained for practical applications.

In stratified condensation flow pattern, the condensed liquid slides smoothly across the inside periphery of the tube wall to create an accumulated bowl-shaped zone at the bottom of the tube cross-section, which is set in an axial motion because of the vapor flow at the upper zone. In contrast, in respect of the film condensate flow, the accumulated liquid stratified layer grows continuously along the tube length [an illustration of the separate zones mentioned above is depicted in Fig. 1(b)].

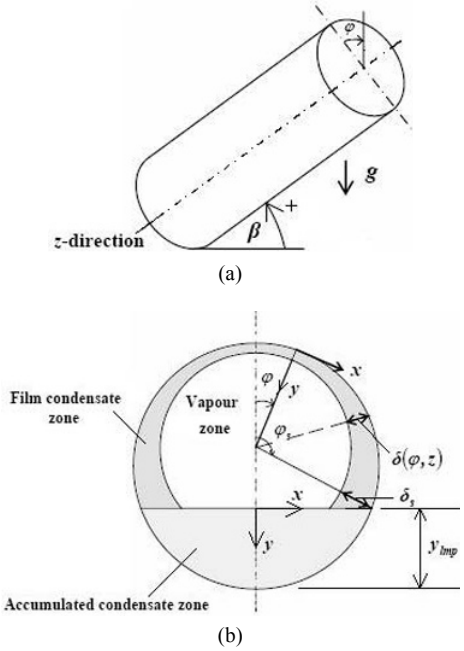

Fig. 1. Physical modeling of stratified condensation in an inclined tube: (a) illustration of an inclined tube and (b) the different zones of vapor and liquid phase distribution during stratified condensation together with their corresponding coordinate systems.

Based on the aforementioned experimental and theoretical studies, the main objectives of this paper are as follows: (1) to develop a physical model and a numerical scheme in order to calculate the stratified condensation local and average heat transfer coefficients for vapor-condensate flow in an inclined tube; (2) to obtain the optimum inclination angle at which the condensation heat transfer coefficient has the highest magnitude; and (3) to compare the obtained results with available published data to validate the accuracy of the present model.

2. Theoretical analysis

2.1 Description of the model

An inclined tube with a very small wall thickness contains vapor flowing inside. The vapor condenses on the tube wall as it proceeds toward the end of the tube. The physical system of film condensation stratified flow inside an inclined tube is illustrated in Fig. 1. Saturated vapor enters the tube at z = 0, and gradually condenses on the subcooled tube wall surface while flowing in the z-direction.

The condensate film is formed on the inside of the tube wall and flows tangentially down along the periphery of the tube in the x-direction. In the resumption, the condensate forms a stratified flow layer at the tube bottom, and this condensate flow is continuously supplemented by the condensate film falling from the upper tube surfaces.

To simplify the analysis, several assumptions are made:

(1) The condensate film flow is assumed to be steady and laminar.

(2) The working fluid is assumed to be pure and Newtonian.

(3) The wall temperature is assumed to be constant and equal to T_w.

(4) The liquid film surface temperature at the liquid-vapor interface is assumed to be constant and equal to the inlet saturation temperature, $T_{sat.}$.

(5) The fluid properties are evaluated at a reference temperature that equals $(T_w + T_{sat.})/2$, and the property variations are neglected, except for the density in the momentum equations (Boussinesq approximation [12]).

(6) The thickness of the condensate film is assumed to be small in comparison to the tube diameter, and the surface tension and curvature effects are neglected.

(7) The condensate film is very thin; thus, the heat is mainly transferred by conduction from the surface of the condensate film to the tube wall. The heat transfer by convection in the liquid film is therefore negligibly small.

(8) The effect of interfacial shear stress on the condensation heat transfer coefficient inside inclined tubes is small in the vapor flow regime [13]. Thus, the interfacial shear stress at the liquid-vapor interface is neglected.

(9) The pressure variations in the condensate film in the axial and peripheral directions in inclined tubes are usually small compared to the viscous forces acting on the liquid film [13]. As a result, the pressure gradient in the liquid film is neglected.

(10) The variations of the axial and tangential velocities in the axial and peripheral directions are negligible compared to their variations in the radial direction.

(11) The inertia forces in the condensate film are neglected in comparison with the viscosity and gravity forces.

(12) The interface between the vapor zone and the accumulated condensate liquid zone is assumed to be smooth and horizontal.

2.2 Condensate film flow analysis, $0 \le \varphi \le \varphi_s$

The equations governing the kinematics, dynamics, and energetic fields of the flow are simplified by using the thin film approximation. The simplified governing equations are given as follows.

Continuity equation:

$$\frac{\partial u}{\partial x} + \frac{\partial w}{\partial z} = 0 \tag{1}$$

X-component of momentum equation:

$$\mu_l \frac{\partial^2 u}{\partial y^2} + (\rho_l - \rho_v) g \sin\phi \cos\beta = 0 \tag{2}$$

Z-component of momentum equation:

$$\mu_l \frac{\partial^2 w}{\partial y^2} + (\rho_l - \rho_v) g \sin\beta = 0 \tag{3}$$

Energy equation:

$$\frac{\partial^2 T}{\partial y^2} = 0 . \tag{4}$$

To complete the formulation, the following boundary conditions are introduced:

$$at \;\; y = 0 \;:\; u = w = 0 \tag{5}$$

$$at \;\; y = \delta \;:\; \begin{cases} \dfrac{\partial u}{\partial y} = \dfrac{\partial w}{\partial y} = 0 \\ T = T_{sat.} \;;\; j_{fl} = -\dfrac{k_l}{\rho_l h_{fg}} \left(\dfrac{\partial T}{\partial y} \right) \end{cases} \tag{6}$$

where j_{fl} is the superficial velocity of the condensate film, given by the following equation:

$$j_{fl} = -\left(u \frac{\partial \delta}{\partial x} + w \frac{\partial \delta}{\partial z} \right)_{y=\delta} . \tag{7}$$

Integrating Eq. (2) across the film thickness with boundary conditions (5) and (6) leads to the following:

$$u = \frac{g(\rho_l - \rho_v)\sin\phi \cos\beta}{\mu_l} \delta^2 \left[\frac{y}{\delta} - \frac{1}{2} \left(\frac{y}{\delta} \right)^2 \right] . \tag{8}$$

Similarly, integrating Eq. (3) with respect to y, together with boundary conditions, yields the z-component velocity profile:

$$w = \frac{g(\rho_l - \rho_v)\sin\beta}{\mu_l} \delta^2 \left[\frac{y}{\delta} - \frac{1}{2} \left(\frac{y}{\delta} \right)^2 \right] . \tag{9}$$

Furthermore, a linear temperature distribution from the integration of Eq. (4) with boundary conditions (5) and (6) is obtained:

$$T = T_w + (T_{sat.} - T_w) y/\delta . \tag{10}$$

The local film thickness equation can be obtained by integrating the continuity equation with respect to y. Thus,

$$\frac{\partial}{\partial x} \int_0^\delta u dy \;\; + \;\; \frac{\partial}{\partial z} \int_0^\delta w dy \;\; = \left(k_l / \rho_l h_{fg} \right) \left(\partial T / \partial y \right)_{y=\delta} \tag{11}$$

where the interfacial mass balance boundary condition, Eq. (6), and the analytic form of condensation rate, Eq. (7), are used. Furthermore, the insertion of Eqs. (8), (9), and (10) for u, w, and T, respectively, into Eq. (11) yields the following partial differential equation for the local film thickness distribution, $\delta(\phi, z)$:

$$\left[\frac{2 g \rho_l (\rho_l - \rho_v) \cos\beta}{\mu_l D} \right] \left(\delta^3 \sin\phi \frac{\partial \delta}{\partial \phi} + \frac{\delta^4}{3} \cos\phi \right) +$$

$$\left[\frac{g\,\rho_l(\rho_l-\rho_v)\sin\beta}{\mu_l}\right]\delta^3\frac{\partial\delta}{\partial z}-\left[k_l\frac{(T_{sat.}-T_w)}{h_{fg}}\right]=0\,. \tag{12}$$

The solution to this partial differential equation can be obtained to yield $\delta=\delta(\phi,z)$, provided that the stratified angle (φ_s) (i.e., the ending value of the peripheral integration limit, $0\le\phi\le\phi_s$, is known). Using a numerical backward finite difference scheme for $(\partial\delta/\partial z)$, the film thickness partial differential equation is reduced to a first-order ordinary differential equation in ϕ. At the tube inlet, z = 0, the film thickness is assumed to be given by the method described in Section 2.2.1, wherein a boundary condition in the z-direction is provided. To be able to solve Eq. (12), we need a second boundary condition to apply in the ϕ-direction. At the top of the tube $(\phi=0)$, the film thickness, $\delta(\phi,z)$, is obtained algebraically from the finite difference form of Eq. (12); consequently, the boundary condition in the ϕ-direction is provided. After the film thickness at the top of the tube is obtained, the film thickness along the perimeter for $0<\phi\le\phi_s$ can be solved by iteration if the local stratified angle (φ_s) is given. Information about this parameter is discussed in Section 2.3.

Boundary condition at the tube inlet cross-section.

The condensate thickness variation function, δ, has its minimum value at the inlet cross-section (i.e., z = 0). Consequently, the partial derivative $\partial\delta/\partial z$ is zero at this location. Hence, rewriting Eq. (12) for the tube inlet cross-section, the third term on the right side of Eq. (12) is omitted, resulting in the following relation:

$$\left[\frac{2\,g\,\rho_l(\rho_l-\rho_v)\cos\beta}{\mu_l D}\right]\left(\delta^3\sin\phi\frac{d\delta}{d\phi}+\frac{\delta^4}{3}\cos\phi\right)-\left[k_l\frac{(T_{sat.}-T_w)}{h_{fg}}\right]=0 \tag{13}$$

Let

$$C\equiv\frac{k_l(T_{sat.}-T_w)\mu_l D}{2\,g\,\rho_l(\rho_l-\rho_v)h_{fg}\cos\beta} \tag{14}$$

Substituting relation (14) into Eq. (13) yields

$$\delta^3\sin\phi\frac{d\delta}{d\phi}+\frac{\delta^4}{3}\cos\phi=C\,, \tag{15}$$

which is a non-linear differential equation. Assuming

$$\xi\equiv\delta^4 \tag{16}$$

Eq. (15) becomes

$$\frac{d\xi}{d\phi}+\frac{4}{3}\frac{\xi}{\tan\phi}=\frac{4C}{\sin\phi}\,. \tag{17}$$

Hence, we reach a linear differential equation of the first order with the following analytic solution:

$$\xi=\frac{4C}{(\sin\phi)^{4/3}}\int(\sin\phi)^{1/3}\,d\phi\,. \tag{18}$$

Therefore,

$$\delta(\phi)=\left[\frac{2\,k_l(T_{sat.}-T_w)\mu_l D}{g\,h_{fg}\,\rho_l(\rho_l-\rho_v)\cos\beta}\right]^{1/4}(\sin\phi)^{-1/3}\left[\int_0^{\phi}(\sin\phi)^{1/3}\,d\phi\right]^{1/4}. \tag{19}$$

This is a beneficial result because this may be used as the boundary condition at the tube inlet cross-section.

2.3 Accumulated condensate flow, $\phi_s<\phi\le\pi$

Up to this point, we have described how, at any point along the tube, the amount of condensate forming on the upper part of the wall cross-section $(0\le\varphi\le\varphi_s)$ can be calculated. This condensate flows down the wall to form the accumulated layer. Considering an arbitrary position z in the axial direction along the tube, Fig. 1 shows the coordinate system in this region. Note that the coordinate system has changed from that used for the condensate film flow.

The total mass flow rate of the liquid condensate per unit length in the axial direction is composed of two parts: one part originates from the thin film condensate layer, and the other part is produced due to the condensing vapor at the interface between the vapor zone and the accumulated condensate zone.

The stratified accumulated layer depth starts at a value that equals the film thickness at an angle ϕ_s and increases to reach a maximum value at the bottom of the tube y_{lmp} at $\phi=\pi$. The values of y_{lmp} are obtained geometrically by the following relation:

$$y_{lmp}=\frac{D}{2}(1+\cos\phi_s)\,. \tag{20}$$

Assuming the condensate layer to be in laminar motion, the continuity and momentum equations are simplified as follows.

Continuity equation:

$$\frac{\partial u_{acc.}}{\partial x}+\frac{\partial w_{acc.}}{\partial z}=0 \tag{21}$$

Z-component of momentum equation:

$$\mu_l\left(\frac{\partial^2 w_{acc.}}{\partial x^2}+\frac{\partial^2 w_{acc.}}{\partial y^2}\right)+(\rho_l-\rho_v)g\sin\beta=0 \tag{22}$$

Let

$$\lambda \equiv \left(\partial^2 w_{acc.}/\partial x^2\right)/\left(\partial^2 w_{acc.}/\partial y^2\right). \quad (23)$$

The thickness of the condensate film is assumed to be small compared to the tube diameter. Hence, $\partial^2 w_{acc.}/\partial y^2 >> \partial^2 w_{acc.}/\partial x^2$ and the ratio λ is much smaller than 1, and can be disregarded. Consequently, Eq. (22) results in a non-partial differential equation:

$$\frac{d^2 w_{acc.}}{dy^2} = -\frac{g(\rho_l - \rho_v)\sin\beta}{\mu_l}. \quad (24)$$

The following boundary conditions apply:

$$\begin{cases} at\ \ y=0 \ \ : \ \ \dfrac{dw_{acc.}}{dy}=0 \\ at\ \ y=y_{lmp} \ \ : \ \ w_{acc.}=0 \end{cases}. \quad (25)$$

Integrating Eq. (24) across the accumulated condensate thickness with respect to y with its corresponding boundary condition equations [i.e., relation (24)] yields the following:

$$w_{acc.} = \frac{g(\rho_l - \rho_v)\sin\beta}{2\mu_l}\left(y_{lmp}^2 - y^2\right). \quad (26)$$

Integrating Eq. (26) across the height of the condensate layer, the average local velocity of the accumulated condensate layer in axial direction is derived as follows:

$$\bar{w}_{acc.} = \frac{1}{y_{lmp}}\int_0^{y_{lmp}} w_{acc.}\, dy = \frac{g(\rho_l - \rho_v)\sin\beta}{3\mu_l}\left(y_{lmp}^2\right). \quad (27)$$

The vapor cross-sectional area is related to the stratified angle of the accumulated layer by the following relation:

$$A_v = \frac{D^2}{8}\left(2\phi_s - \sin 2\phi_s\right). \quad (28)$$

If we assume that the cross-sectional area of the condensate in the film region is negligible, we have the following relation for the liquid cross-sectional area:

$$A_{acc.} = \frac{D^2}{8}\left(2\pi - 2\phi_s + \sin 2\phi_s\right). \quad (29)$$

With the aid of relations (27) and (29), the condensate mass flow rate can be calculated using the following relation:

$$\dot{m}_{acc.} = \rho_l A_{acc.} \bar{w}_{acc.}. \quad (30)$$

From the equations listed above, all the needed design parameters can be calculated, provided that the stratified angle of the accumulated layer at each cross-section is known from the data obtained at the previous section. However, at the first step, there is no "previous section." Hence, in order to be able to start the calculation procedure, a stratified angle for the first section should be assumed to follow the path from that point on. As such, the question that comes to mind is "What is the guarantee that the assumed angle is the proper value at the first step?" Hence, an extra relationship is needed to serve as the checkpoint for the assumption. The only means to find such a relationship is to search the literature and choose a correlation that best fits the special circumstances of the field under investigation.

The relationship chosen for this study is the following [14]:

$$\dot{m}_{acc.} = (0.00127)\frac{g\rho_l^2 D^4 \sin\beta}{\mu_l}\left(\pi - \phi_s\right)^{7.0423}. \quad (31)$$

This is suitable for laminar, stratified flow of common fluids (e.g., water and the refrigerants group).

2.4 Heat transfer coefficient

With the calculated thickness of the condensate at each cross-section, $\delta(\phi, z)$, the local, averaged local, and overall heat transfer coefficients are obtained by the following equations.

I) Condensate film flow region, $0 \le \phi \le \phi_s$:

The local heat transfer coefficient of the condensate thin film,

$$h_1(\phi, z) = \frac{k_l}{\delta(\phi, z)} \quad (32)$$

and its averaged local heat transfer coefficient,

$$h_1(z) = \frac{1}{\phi_s}\int_0^{\phi_s} h_1(\phi, z)\, dz. \quad (33)$$

II) Accumulated condensate flow region, $\phi_s < \phi \le \pi$:

The heat transfer coefficient for the accumulated condensate flow is negligibly small compared to the heat transfer coefficient, h1, for the film condensate flow. In almost all analyses associated with condensation in tubes, the contribution of the accumulated condensate flow to the overall heat transfer coefficient at any axial distance, z, is completely neglected. The averaged local value of heat transfer coefficient for the accumulated region at an arbitrary cross-section in the z-direction is equal to the following:

$$h_2(z) = \frac{k_l}{y_{lmp}(z)}. \quad (34)$$

III) Summing up the separate relations in the regions (I) and (II) listed above, we obtain the averaged local heat transfer coefficient for an arbitrary cross-section in the z-direction:

$$h_m(z) = \frac{\phi_s(z)}{\pi}h_1(z) + \left[1 - \frac{\phi_s(z)}{\pi}\right]h_2(z). \quad (35)$$

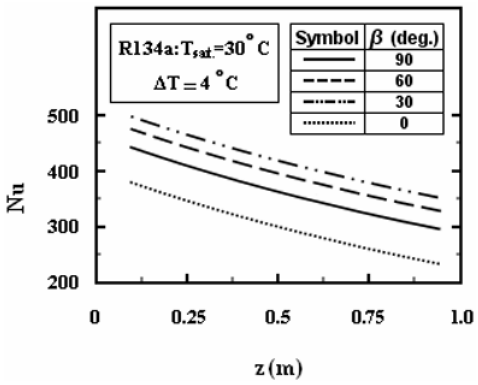

(a) $Re_{v,i}=4\times10^4$

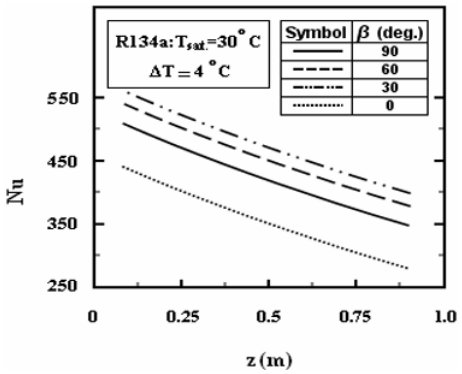

(b) $Re_{v,i}=6\times10^4$

Fig. 2. Variation of the averaged local Nusselt number along the tube length for different inclination angles and vapor inlet Reynolds numbers: (a) $Re_{v,i} = 4 \times 10^4$ and (b) $Re_{v,i} = 6 \times 10^4$.

IV) Finally, the mean overall condensation heat transfer coefficient for the entire tube surface is obtained as follows:

$$h_{m,o} = \frac{1}{L}\int_0^L h_m(z)\,dz\,. \tag{36}$$

3. Results and discussion

The variation of the averaged local dimensionless Nusselt number along the tube length at various inclination angles while keeping the vapor inlet Reynolds number, $Re_{v,i}$, saturation temperature, $T_{sat.}$, and subcooling temperature difference, ΔT, constant is depicted in Fig. 2. Due to the relatively higher vapor flow rates at the entry region of the tube, the rate of the heat transfer and, consequently, the magnitude of the Nusselt number are the highest at the tube inlet. Furthermore, because of the uniform conversion of the vapor phase into the liquid phase, a gradual decrease in the magnitude of the Nusselt number is observed for all inclination angles. According to Eq. (12), both gravitational and viscous forces affect the thermal and hydrodynamic behaviors of the condensation phenomenon in the inclined tubes. However, while the gravitational force helps the heat transfer coefficient to increase in magnitude, the viscous force reduces the amount of the heat transfer coefficient by opposing the fluid flow and increasing the thickness of the condensate liquid film. As a result, by altering the tube inclination angle between horizontal and vertical orientations, the heat transfer coefficient (and, correspondingly, the Nusselt number) reaches its maximum amount at an optimum inclination angle, after which the magnitude of the heat transfer coefficient starts to decrease. The location of this "optimum angle" depends heavily on the physical and thermal properties of the flow. Hence, there is a specific optimum inclination angle in any condition. Considering the saturation and subcooling temperature difference of 30 and 4 °C, respectively, with R134a as the working fluid and an inlet vapor Reynolds number of 4×10^4, at the inclination angle $\beta = 30°$, the Nusselt numbers are 35% and 14% greater than its corresponding magnitudes for horizontal and vertical orientations, respectively. Moreover, the Nusselt number is 5% more than its magnitude at $\beta = 60°$. The parametric effect of the vapor inlet Reynolds number on the axial variation of the Nusselt number is also demonstrated in Figs. 2(a) and 2(b). As indicated by the curves in these figures, higher vapor inlet Reynolds numbers yield higher Nusselt numbers because of the corresponding increase in the mass velocity of the vapor phase.

According to Eq. (32), an increase in the magnitude of the thickness of the condensate liquid film is an indicator of the reduction in the magnitude of the heat transfer coefficient. Fig. 3 presents the variations of the condensate film thickness along the tube periphery for two inclination angles, 30° and 60°, at the axial position of 0.3 m with $Re_{v,i} = 4 \times 10^4$. Increasing the inclination angle from 30° to 60° results in an increase in the magnitude of the condensate liquid film thickness, which is in agreement with the reduction of the heat transfer coefficient illustrated previously in Fig. 2.

The variation of the liquid condensate film thickness along the tube periphery at different axial positions while keeping the inclination angle and the inlet vapor Reynolds number constant is illustrated in Fig. 4, where $\beta = 30°$ and $Re_{v,i} = 4 \times 10^4$. The film thickness for the condensation of saturated vapor inside an inclined tube increases, not only along the peripheral direction (Fig. 3), but also along the axial coordinate, with the progress of condensation along the tube. This results in increasing thermal resistance to heat flow from vapor to the cooling region and, consequently, a reduction of the heat transfer rate. The peripheral angle at which the condensate film thickness approaches its limiting value is a representative of the stratified angle and the entrance to the accumulated condensate region. Increasing the axial position yields a thicker accumulated condensate layer or a smaller stratified angle. In Fig. 5, for instance, the stratified angle decreases from 174° at the axial position z = 0.1 m to 166° at z = 0.4 m. Additionally, according to Fig. 5, as the inclination angle changes from $\beta = 30°$ to $\beta = 60°$, the stratified angle decreases because of the increase in the condensate liquid thickness.

The variations of the averaged local heat transfer coefficient along the tube length considering the effects of the saturation temperature and the subcooling temperature difference for two

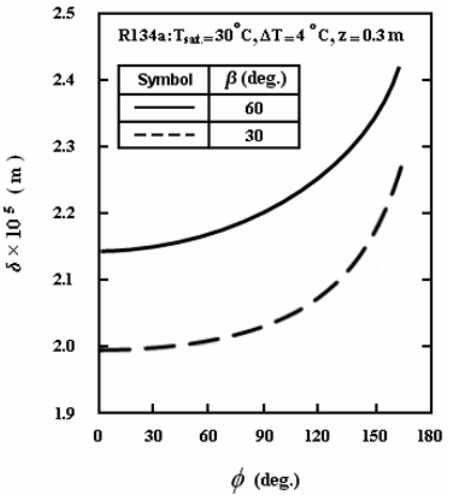

Fig. 3. Development of the condensate film thickness along the tube periphery at different inclination angles.

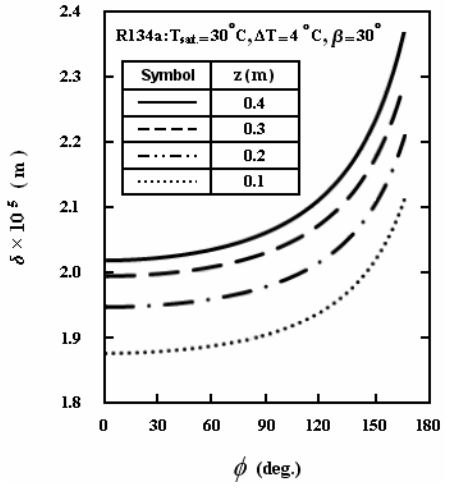

Fig. 4. Development of the condensate film thickness along the tube periphery at different axial positions.

different inclination angles are illustrated in Figs. 6 and 7, respectively. According tothese figures, increasing the saturation temperature results in higher heat transfer coefficients, whereas increasing the subcooling temperature difference decreases the heat transfer coefficient. The reason behind this behavior is related to the corresponding condensate film thickness development. Both increasing the saturation temperature and decreasing the subcooling temperature difference enhance the development of the condensate film thickness, and allow the heat transfer phenomenon to occur in a smaller area, which correspondingly lead to a higher heat transfer coefficient.

The variation of the overall mean condensation heat transfer coefficient with inlet vapor mass velocity for different inclination angles is depicted in Fig. 8. The overall mean heat transfer coefficient is significantly influenced by the inclination angle. Owing to the increase in vapor velocity per unit cross-sectional area, the heat transfer rate increases, resulting in

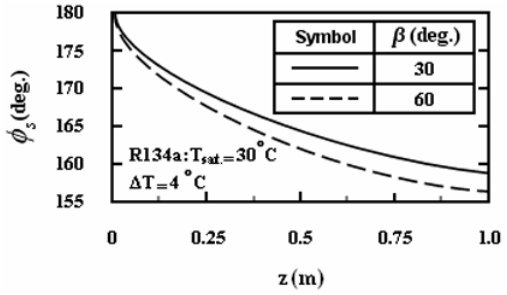

Fig. 5. Variation of the stratified angle along the tube length at different inclination angles.

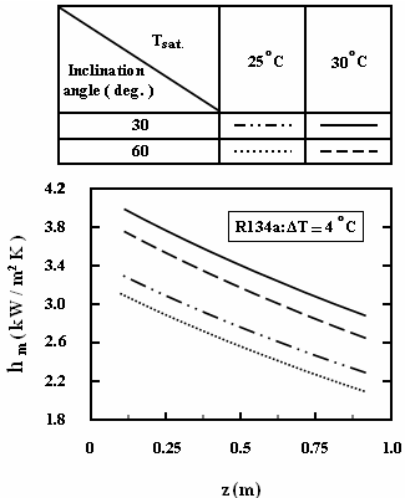

Fig. 6. Variation of the averaged local condensation heat transfer coefficient along the tube length for different inclination angles and vapor saturation temperatures.

higher heat transfer coefficients. The mean heat transfer coefficient at the inclination angle β = 30° is found to have the highest magnitude compared with β = 60° and the vertical orientation. In the resumption, the results of the present study for the overall mean heat transfer coefficient are compared with the magnitudes obtained by the following semi-empirical relation proposed by Wang and Yiwei [15]:

$$\frac{h_{m,o}}{h_{Nu}} = \left(\frac{2L}{D}\right)^{\frac{\cos\beta}{4}} \left(0.54 + 5.86\times10^{-3}\beta\right) \tag{37}$$

where h_{Nu} is the Nusselt condensation heat transfer coefficient [16]:

$$h_{Nu} = 0.943\left[\frac{\rho_l^2 g h_{fg} k_l^3 \sin\beta}{L\mu_l \Delta T}\right]^{1/4} \tag{38}$$

Fig. 8 shows that the predictions of the present study have developed in the same way as the data obtained by the Wang and Yiwei relation, showing a good consistency between them for all inclination angles.

Figs. 9, 10 and 11 represent the effect of the inclination angle variation on the mean overall condensation heat transfer

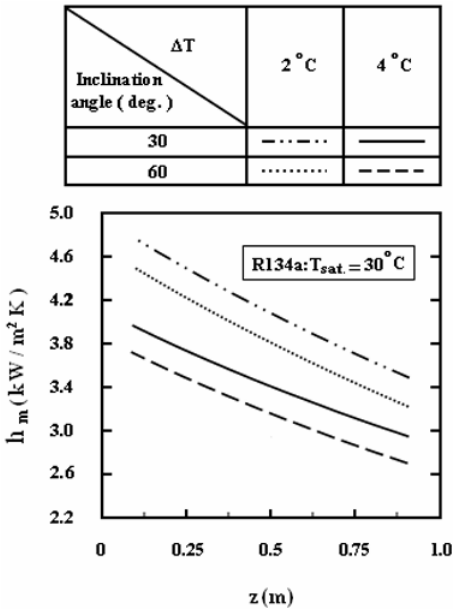

Fig. 7. Variation of the averaged local condensation heat transfer coefficient along the tube length for different inclination angles and subcooling temperature differences.

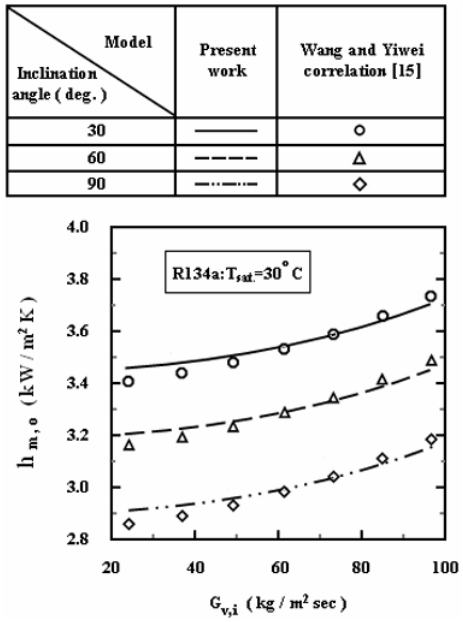

Fig. 8. Variation of the mean overall heat transfer coefficient with vapor inlet cross-section mass velocity for different inclination angles.

coefficient for a tube of length L = 0.6 m and inside diameter of D = 14.3 mm, with R141b, R11, and R134a as the working fluids, respectively. As mentioned previously, as the orientation of the tube is altered between the horizontal and vertical positions, the magnitude of the condensation heat transfer coefficient first experiences a "rise" up to an optimum inclination angle, and then starts to decrease because of the reverse effects of the gravitational and viscous forces. According to the results obtained from the present work for R141b and R11 under the mentioned conditions, a range of inclination angles of between 30° and 40° from the horizontal position yields the highest magnitudes of condensation heat transfer coefficient; however, for R134a, a range of inclination angles of between 40° and 50° yields the highest magnitudes of heat transfer coefficient. This indicates that the optimum inclination angle is dependent on the physical and thermal conditions of the condensing flow.

Again, as mentioned above, the change of magnitudes of condensation heat transfer coefficient is considerable according to the inclination angle. For instance, as Fig. 10 illustrates, at the inclination angle $\beta = 35°$, the mean overall condensation heat transfer coefficient is 41% greater than its magnitude at the horizontal position for R141b as the working fluid.

The results of the present theoretical study for R141b and R11 are compared with the results of the experimental investigation conducted by Cho and Han [11]. A good agreement is observed between the results for both working fluids.

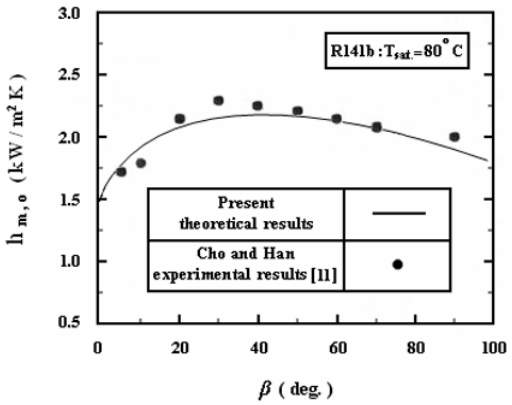

Fig. 9. Comparison of the present theoretical analysis mean overall condensation heat transfer coefficient with experimental data [11] for refrigerant R141b.

4. Conclusions

A theoretical analysis, together with a numerical solution, has been carried out for the purpose of predicting heat transfer coefficient for condensation inside inclined tubes. The analysis takes into account the effects of the saturation temperature level, subcooling temperature difference, inlet vapor Reynolds number and mass velocity, and the development of the stratified angle associated with the accumulated condensate layer at the bottom of the tube. The inclination angle has been concluded to be a significant influence on the condensation heat transfer coefficient. The 30–50° range from the horizontal position has also been observed to be the optimum inclination angle for refrigerants R141b, R11, and R134a, which are the working fluids in the conditions considered in the present study. Comparing the results of this study with experimental data, a good agreement is observed between them.

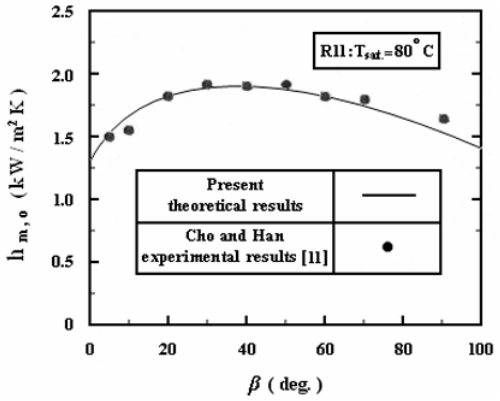

Fig. 10. Comparison of the present theoretical analysis mean overall condensation heat transfer coefficient with experimental data [11] for refrigerant R11.

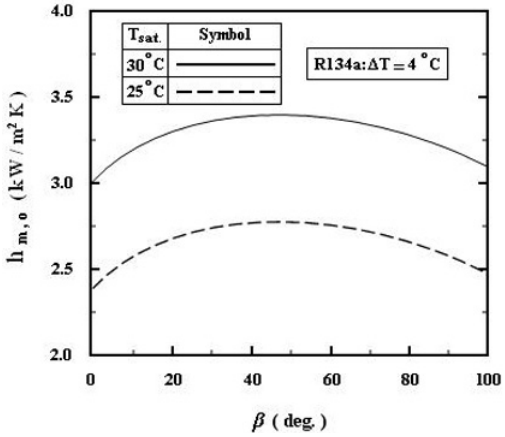

Fig. 11. Variation of the present theoretical analysis mean overall condensation heat transfer coefficient with inclination angles for refrigerant R134a.

Nomenclature

A	:	Cross-sectional area, m^2
C	:	Variable defined by Eq. (14), m^4
D	:	Tube diameter, m
g	:	Gravity acceleration, m/s^2
G	:	Mass velocity, mass flow rate per unit cross-sectional area, kg/ (m^2 sec)
h_1	:	Heat transfer coefficient of the condensate film, W/ (m^2 K)
h_2	:	Heat transfer coefficient of the accumulated condensate layer, W/ (m^2 K)
h_{fg}	:	Latent heat of condensation, J/kg
h_m	:	Averaged local heat transfer coefficient, W/ (m^2 K)
$h_{m,o}$	:	Mean overall heat transfer coefficient for the whole tube surface, W/ (m K)
h_{Nu}	:	Nusselt condensation heat transfer coefficient, J/kg
j_{fl}	:	Superficial velocity of the condensate film, m/s
k	:	Thermal conductivity, W/ (m K)
L	:	Tube length, m
$\dot{m}$	:	Mass flow rate, kg/s
Nu	:	Averaged local Nusselt number ($\equiv h_m D / k_l$)
T	:	Temperature, K
$Tsat.$	:	Saturation temperature, K
Tw	:	Wall temperature, K
ΔT	:	Temperature difference ($\equiv T_{sat.} - T_w$)
u, w	:	Velocity components in x- and z- directions, respectively, m/s
x, y, z	:	Fundamental coordinate system, m
y_{lmp}	:	Accumulated condensate layer lowermost point height, m

Greek symbols

β	:	Angle of inclination of tube with respect to the horizontal axis, rad
δ	:	Film condensate thickness, m
λ	:	Variable defined by Eq. (23), dimensionless
μ	:	Dynamic viscosity, kg/ (m s)
ξ	:	Variable defined by Eq. (16), m^4
ρ	:	Density, kg/m^3
ϕ	:	Peripheral angle, rad
ϕ_s	:	Stratified angle of the accumulated layer, rad

Superscripts

-	:	Average value

Subscripts

acc.	:	Accumulated condensate layer

References

[1] H. D. Baehr and K. Stephan, *Heat and mass transfer*, Springer, Berlin, Germany (2006).

[2] S. M. Ghiaasiaan, *Two-phase flow, boiling and condensation in conventional and miniature systems*, Cambridge University Press, New York, USA (2008).

[3] J. G. Collier and J. R. Thome, *Convective boiling and condensation,* Oxford University Press, Oxford, UK (1996).

[4] A. Cavallini, G. Censi, D. D. Col, L. Doretti, G. A. Longo, L. Rossetto and C. Zilio, Condensation inside and outside smooth and enhanced tubes – a review of recent research. *International Journal of Refrigeration,* 26 (4) (2003) 373-392.

[5] A. S. Dalkilic and S. Wongwises, Intensive literature review of condensation inside smooth and enhanced tubes. *International Journal of Heat and Mass Transfe*r, 52 (15, 16) (2009) 3409-3426.

[6] H. S. Wang and J. W. Rose, Film Condensation in Microchannels: Effect of Tube Inclination. *Proceedings of the 4th International Conference on Nanochannels, Microchannels and Minichannels*, ASME, Limerick, Ireland, CD, paper ICNMM2006-96049 (2006).

[7] T. Nitheanandan and H. M. Soliman, Influence of tube inclination on the flow regime boundaries of condensing steam.

Canadian Journal of Chemical Engineering, 71 (1) (1993) 35-41.

[8] G. P. Fieg, Calculation of laminar film condensation in/on inclined elliptical tubes. *International Journal of Heat and Mass Transfer,* 37 (4) (1994) 619-624.

[9] H. M. S. Hussein, M. A. Mohamad and A. S. El-Asfouri, Theoretical analysis of laminar-film condensation heat transfer inside inclined wickless heat pipes flat-plate solar collector. *Renewable Energy*, 23 (3, 4) (2001) 525-535.

[10] K. Han, S. Yee, S. Park, S. Lee and D. Cho, A study on the improvement of heat transfer performance in low temperature closed thermosyphon. *KSME International Journal,* 16 (9) (2002) 1102-1111.

[11] D. Cho and K. Han, Influence of the inclination angle and liquid charge ratio on the condensation in closed two-phase thermosyphons with axial internal low-fins. *KSME International Journal*, 17 (3) (2003) 422-428.

[12] A. Bejan, *Convection Heat Transfer*, John Wiley and Sons, New York, USA (2004).

[13] S. Chen, J. Reed and L. Tien, Reflux condensation in a two-phase closed thermosyphon. *International Journal of Heat and Mass Transfer,* 27 (9) (1984) 1587–1594.

[14] J. S. Lioumbas, S. V. Paras and A. J. Karabelas, Co-current stratified gas–liquid downflow—Influence of the liquid flow field on interfacial structure. *International Journal of Multiphase Flow,* 31 (8) (2005) 869-896.

[15] J. C. Y. Wang and M. Yiwei, Condensation heat transfer inside vertical and inclined thermosyphons. *Journal of heat transfer*, 113 (1991) 777-780.

[16] W. Nusselt, Die Ooberflachen-Kondensation des Waserdampfes. *Zeitschr.* V.D.I. 60 (1916) 541-569.

Hamid Saffari received his Ph.D. degree from Moscow Power Engineering Institute, Russia. Dr. Saffari is currently an Assistant Professor at the School of Mechanical Engineering at Iran University of Science and Technology. His research interests include two-phase flow and HVAC&R.